Sources of C_2–C_4 alkenes, the most important ozone nonmethane hydrocarbon precursors in the Pearl River Delta region

CrossMark

Yanli Zhang [a], Xinming Wang [a,*], Zhou Zhang [a,b], Sujun Lü [a,b], Zhonghui Huang [a,b], Longfeng Li [a,c]

[a] State Key Laboratory of Organic Geochemistry, Guangzhou Institute of Geochemistry, Chinese Academy of Sciences, Guangzhou 510640, China
[b] University of Chinese Academy of Sciences, Beijing 100049, China
[c] School of Chemistry and Material Sciences, Huaibei Normal University, Huaibei 235000, China

HIGHLIGHTS

- C_2–C_4 alkenes shared 11–20% in mixing ratios but 38–64% OFPs by NMHCs.
- Vehicle exhausts contributed most to ethylene (32–49%) and propene (35–41%).
- LPG contributed most to butenes (38–65%) and largely to propene (23–36%).
- Reducing alkene contents in LPG would benefit regional surface ozone control.

ARTICLE INFO

ABSTRACT

Surface ozone is becoming an increasing concern in China's megacities such as the urban centers located in the highly industrialized and densely populated Pearl River Delta (PRD) region, where previous studies suggested that ozone production is sensitive to VOC emissions with alkenes being important precursors. However, little was known about sources of alkenes. Here we present our monitoring of ambient volatile organic compounds at four representative urban, suburban and rural sites in the PRD region during November–December 2009, which experienced frequent ozone episodes. C_2–C_4 alkenes, whose total mixing ratios were 11–20% of non-methane hydrocarbons (NMHCs) quantified, accounted for 38–64% of ozone formation potentials (OFPs) and 30–50% of the total hydroxyl radical (OH) reactivity by NMHCs. Ethylene was the most abundant alkene, accounting for 8–15% in total mixing ratios of NMHCs and contributed 25–46% of OFPs. Correlations between C_2–C_4 alkenes and typical source tracers suggested that ethylene might be largely related to vehicle exhausts and industry activities, while propene and butenes were much more LPG-related. Positive Matrix Factorization (PMF) confirmed that vehicle exhaust and liquefied petroleum gas (LPG) were two major sources that altogether accounted for 52–62%, 58–77%, 73–83%, 68–79% and 73–84% for ethylene, propene, 1-butene, trans-2-butene and cis-2-butene, respectively. Vehicle exhausts alone contributed 32–49% ethylene and 35–41% propene. Industry activities contributed 13–23% ethylene and 7–20% propene. LPG instead contributed the most to butenes (38–65%) and substantially to propene (23–36%). Extensive tests confirmed high fractions of propene and butenes in LPG then used in Guangzhou and in LPG combustion plumes; therefore, limiting alkene contents in LPG would benefit regional ozone control.

© 2014 Elsevier B.V. All rights reserved.

1. Introduction

Tropospheric ozone is formed from the photochemical reactions of volatile organic compounds (VOCs) and nitrogen oxide (NO_x) in the presence of sunlight (Haagen-smit and Fox, 1956; Finlayson-Pitts, 2010). As a key trace constituent in the troposphere, ozone plays a vital role in controlling the chemical composition of the troposphere (Logan, 1985). Ozone is also a greenhouse gas that directly contributes to global warming and influences the radiative balance of the upper troposphere and lower stratosphere (IPCC, 2007). Ozone near the ground is a hazardous air pollutant that not only has adverse health effects (Lippmann, 1989; Beckett, 1991), but also impacts heavily on crop yields and plant growth (Lippmann, 1989; Chameides et al., 1994; Wang et al., 2007a,b). Combating surface ozone has long been a formidable task since heavy photochemical smog occurred in Los Angeles in the 1940s. While there are still nonattainment areas for ozone in developed countries like the USA (Hakami et al., 2006), in the developing world ozone pollution is becoming an air quality issue of increasing concern, particularly in megacities and their downwind regions (Beig and

Singh, 2007; Kulkarni et al., 2010; Lal et al., 2012). In south China's Pearl River Delta region, for example, observed ambient ozone levels frequently exceeded the guideline level of 200 μg/m³ or 102 ppbv (1-h average; GB 3095-2012) (Wang et al., 2003; Lam et al., 2005; Zheng et al., 2010), and even background ozone levels have increased steadily in recent years (Chan et al., 2003; Wang et al., 2009).

Developing ozone control strategies is very difficult since ozone does not respond in a proportional manner to reductions in the precursor emissions (Finlayson-Pitts and Pitts, 1999). Understanding the complex nonlinear O_3-VOC-NOx chemistry, which is a prerequisite for formulating control strategies (Dodge, 1977; Finlayson-Pitts and Pitts, 1993), is usually simplified to display in the form of 2-dimensional isopleths such as the Empirical Kinetic Modeling Approach (EKMA) model (Martinez et al., 1983). Although the VOC-limited region is found in highly polluted urban areas while the NO_x-control is typical of downwind suburban and rural areas (Finlayson-Pitts and Pitts, 1993), the diagnostics of ozone production regime is not always obvious. A recent study by Liu et al. (2012), with a comprehensive photochemical modeling analysis based on measurements in Beijing, demonstrated that ozone production might be in a transition regime where it is sensitive to both VOC and NO_x emissions. As for the PRD region, previous studies revealed that ground-level ozone production was sensitive to VOC emissions (Zhang et al., 2007; Shao et al., 2009; Cheng et al., 2010), and aromatic hydrocarbons (AHs) and alkenes were the critical VOC groups contributing to ozone formation (Tang et al., 2007; Zhang et al., 2007; Cheng et al., 2010; Y.L. Zhang et al., 2012). Therefore reduction of AHs and alkenes is vital for ozone pollution control in the region and knowing their sources is the first step toward this reduction. Sources of AHs in the PRD regions were previously explored by applying receptor models with monitoring data, such as PCA/APCS method by Guo et al. (2006), chemical mass balance (CMB) technique by Liu et al. (2008a), and the Positive Matrix Factorization (PMF) method by Zhang et al. (2013a). By tightening the control of oil-based solvents in the region, emission of AHs from the industry sector should decrease AH levels in the region; alkenes, another important group of ozone precursors, would be instead becoming more distinctive in the formation of ozone. Yet sources of alkenes in this region have been rarely investigated, partly because they are even more reactive than AHs and therefore apportioning their sources based on monitoring data is more challenging.

In the present study, ambient air samples were collected during November to December in 2009 at representative urban, suburban, and rural sites in the PRD region. The objectives were to obtain extensive data to re-assess the role of alkenes among VOCs to form ozone, to identify major sources of alkenes by typical source tracers and to explore source contributions by using a PMF receptor model.

2. Field sampling and lab works

2.1. Site description and field sampling

Four sampling sites were selected for this campaign and their geographical locations are shown in Fig. 1. These four sites are all air quality monitoring stations established by the local government environmental monitoring center. Their details are listed in Table 1.

Previous studies on the seasonal variations of ozone in the PRD region revealed that higher levels typically occurred in October, November and December (Wang et al., 2009). In the present study we collected ambient air samples during November–December, 2009, using pre-evacuated 2-l electro-polished stainless steel canisters. The maximum 1-h ozone concentration values during the sampling period frequently exceeded the guideline level of 200 μg/m³, particularly downwind the urban centers. For example, in November 2009 the maximum 1-h ozone concentrations reached as high as 202 μg/m³ at GEMC and 407 μg/m³ at WQS. Samples were collected only on sunny/cloudy days not on rainy days. During field sampling a flow restrictor (Part No. 39-RS-3, Entech Instruments Inc., CA, USA) was adopted to allow each canister to be filled in about 60 min. During this campaign, altogether 233 air samples were collected including 67 samples from
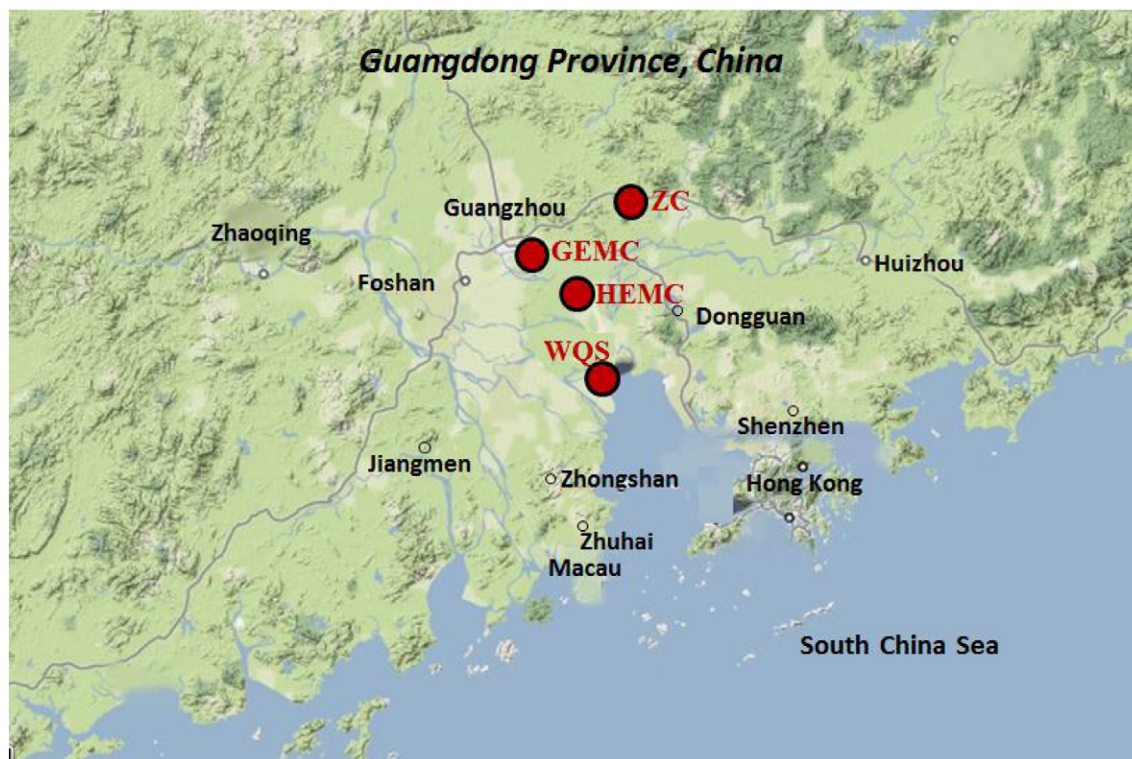
Fig. 1. Sampling sites in the PRD region, China. GEMC: Guangzhou Environmental Monitoring Center (urban); HEMC: Higher Education Mega Center (suburban); ZC: Zengcheng College of South China Normal University (upwind rural); and WQS: Wanqingsha town (downwind rural).

Table 1
Description of sampling sites.

Sampling sites	Type	Location	Sampling height	Surrounding
Guangzhou Environmental Monitoring Center (GEMC)	Urban	23.13°N, 113.27°E	23 m	In the center of Guangzhou city with intensive residential buildings and business offices; highly influenced by traffic-related and residential emission sources.
Guangzhou Higher Education Mega Center (HEMC)	Suburban	23.04°N, 113.37°E	20 m	In an island in the middle of the Pearl River in the southern part of Panyu district; about 17 km to the southeast of urban Guangzhou and 40 km to the northwest of Dongguan. The island hosts ten universities without agricultural or industrial activities.
Zengcheng College of South China Normal University (ZC)	Rural/upwind	23.31°N, 113.56°E	15 m	In the northeast of urban Guangzhou; surrounded by farmlands; upwind of urban Guangzhou during our sampling period.
Wanqingsha (WQS)	Rural/downwind	22.71°N, 113.55°E	15 m	In a small town in the center of the PRD region; surrounded by farmlands with very few textile and clothing workshops in the neighborhood; 50 km to the southeast of Guangzhou urban center, 40 km to the southwest of Dongguan; downwind Dongguan and/or Guangzhou during our sampling period.

GEMC, 51 samples from HEMC, 41 samples from ZC and 74 samples from WQS.

2.2. Lab analysis

Air samples were analyzed using a Model 7100 Preconcentrator (Entech Instruments Inc., California, USA) coupled with an Agilent 5973N gas chromatography-mass selective detector/flame ionization detector (GC-MSD/FID, Agilent Technologies, USA). Detailed cryogenically concentration steps are described elsewhere (Zhang et al., 2013a). Briefly, VOCs inside the canisters were initially concentrated using liquid-nitrogen cryogenic trap at −160 °C. The trapped VOCs were then transferred by pure helium to a secondary trap at −40 °C with Tenax-TA as adsorbent. The majority of H_2O and CO_2 were removed during these two steps. The secondary trap was then heated to get VOCs transferred by helium to a third cryo-focus trap at −170 °C. After the focusing step, the trap was rapidly heated and the VOCs were transferred to the GC-MSD/FID system. The mixture was firstly separated by a HP-1 capillary column (60 m × 0.32 mm × 1.0 μm, Agilent Technologies, USA) with helium as carrier gas, and then split into two: one is to a PLOT-Q column (30 m × 0.32 mm × 2.0 μm, Agilent Technologies, USA) followed by FID detection; another is to a 65 cm × 0.10 mm I.D. stainless steel line followed by MSD detection. The GC oven temperature was programmed to be initially at −50 °C, holding for 3 min; increasing to 10 °C at 15 °C min^{-1}, then to 120 °C at 5 °C min^{-1}, and then to 250 °C at 10 °C min^{-1} and holding for 10 min. The MSD was used in selected ion monitoring (SIM) mode and the ionization method was electron impacting (EI).

2.3. Quality control and quality assurance

Before sampling, all canisters were flushed at least five times by repeatedly filling and evacuating humidified zero air. In order to check if there was any contamination in the canisters, all canisters were evacuated after the cleansing procedures, re-filled with pure nitrogen, stored in the laboratory for at least 24 h, and then analyzed the same way as field samples to make sure that all the target VOC compounds were not present.

Target compounds were identified based on their retention times and mass spectra, and quantified by external calibration method. C_4–C_{10} hydrocarbons were determined based on MSD signals, while C_2 and C_3 hydrocarbons were determined based on FID signals. The calibration standards were prepared by dynamically diluting the 100 ppbv Photochemical Assessment Monitoring Stations (PAMS) standard mixture and TO-14 standard mixture (39 compounds) from Spectra Gases Inc., NJ, USA to 0.5, 1, 5, 15 and 30 ppbv. The calibration curves were obtained by running the five diluted standards plus humidified zero air the same way as the field samples. The analytical system was challenged daily with a one-point (typically 1 ppbv) calibration before running air samples. If the response was beyond +/−10% of the initial

calibration curve, recalibration was performed. The method detection limits (MDLs) for each aromatic hydrocarbon were presented in Table 2. The measurement accuracy and precision for C_2–C_4 alkenes are within 5% and 3%, respectively.

2.4. Source apportionment with Positive Matrix Factorization (PMF)

USEPA PMF 3.0 model (http://www.epa.gov/heasd/products/pmf/pmf.html) was applied to explore the sources of observed NMHCs in the present study. The detailed method description can be found elsewhere (Paatero and Tapper, 1994; Paatero, 1997). The approaches for replacing and developing uncertainty values for missing and below-detection-limit data were drawn from previous work (Poirot et al., 2001; Hopke et al., 2003). Briefly, data values below the method detection limit (MDL) were substituted with MDL/2; missing data values were substituted with median concentrations (Brown et al., 2007). Uncertainties were treated the same way as Polissar et al. (1998) and Reff et al. (2007). If the concentration is less than or equal to the MDL provided, the uncertainty is calculated using the following equation, Unc = 5 / 6 ×MDL; if the concentration is greater than the MDL provided, the calculation is Unc = [(Error Fraction × mixing ratios)^2 + (MDL)^2]$^{1/2}$. Most species had all concentration levels above the MDLs. Only four species (n-heptane, 1-pentene, 2-methyl-1-butene, o-ethyltoluene) had concentration levels below MDL at a few samples but the percentages of this kind of samples were all less than 5%. The number of factors in the PMF model was chosen based on the result from PCA/APCS model (Anderson et al., 2001).

3. Results and discussion

3.1. Mixing ratios and compositions of alkenes

In group compositions, total mixing ratios of alkenes ranked second after alkanes at GEMC, HEMC and ZC (Fig. 2), and shared fractions of 11.2%, 17.7%, and 22.0% in NMHCs, respectively. At WQS, however, alkenes became the third group after alkanes (49.1%) and aromatics (28.3%), contributing 12.3% in total mixing ratios of NMHCs. Since C_2–C_4 alkenes shared 91–94% of total alkenes in this study, here we focus only on C_2–C_4 alkenes. Table 2 lists the average mixing ratios and their 95% confidence intervals (95% C.I.) for the major alkenes observed at the four sites. Their method detection limits (MDL), maximum incremental reactivity (MIR) and ozone formation potentials (OFPs), rate constants with OH (K_{OH}) and lifetimes were also showed in Table 2. Obviously, C_2–C_4 alkenes are highly reactive with very short lifetimes (2.2–16.3 h). The mixing ratios of C_2–C_4 alkenes at GEMC, HEMC, ZC and WQS totaled 8.3 ± 1.1, 7.7 ± 1.4, 5.1 ± 1.0, and 5.0 ± 0.5 ppbv, accounting for 10.5%, 16.4%, 20.0%, and 11.2% of the total NMHCs, respectively. Ethylene was the most abundant alkenes at all four sampling sites, 8–15% of total mixing ratios of NMHCs. Mixing ratios of ethylene at urban GEMC (5.7 ± 0.7 ppb) were significantly higher ($p < 0.01$) than those at

Table 2
Mixing ratios (ppb) and 95% confidence intervals (95% C.I.) of major alkenes, as well as their percentages in NMHCs and OFPs (ppb).

Sampling sites		Ethylene	Propylene	1-Butene	trans-2-Butene	cis-2-Butene	Total C_2–C_4 alkenes
	MDL	41	31	17	13	11	
	MIR[a]	7.4	9.4	8.9	10.0	10.0	
	$K_{OH} \times 10^{12}$ (cm^3 molecule^{-1} s^{-1})[b]	8.5	26.3	31.4	64.0	56.4	
	Lifetime (h)[c]	16.3	5.3	4.4	2.2	2.5	
GEMC (n = 69)	Mean mixing ratios ± 95% C.I. (ppb)	5.7 ± 0.7	1.5 ± 0.3	0.5 ± 0.05	0.3 ± 0.03	0.2 ± 0.02	8.3
	Mixing ratios percentage (%)	7.3	1.9	0.6	0.3	0.3	10.5
	OFP ± 95% C.I. (ppb)	**46.9 ± 6.9**	**16.1 ± 3.0**	**4.8 ± 0.5**	**3.3 ± 0.4**	**3.3 ± 0.4**	**74.4**
	OFP percentage (%)	**29.9**	**10.3**	**3.0**	**2.1**	**2.1**	**47.4**
HEMC (n = 52)	Mean mixing ratios ± 95% C.I. (ppb)	5.0 ± 0.8	1.5 ± 0.4	0.6 ± 0.08	0.3 ± 0.05	0.3 ± 0.04	7.7
	Mixing ratios percentage (%)	10.7	3.2	1.3	0.7	0.6	16.4
	OFP ± 95% C.I. (ppb)	**43.6 ± 7.2**	**16.9 ± 4.5**	**5.8 ± 0.8**	**4.2 ± 0.8**	**4.2 ± 0.6**	**74.7**
	OFP percentage (%)	**33.4**	**13.0**	**4.4**	**3.3**	**3.2**	**57.3**
ZC (n = 41)	Mean mixing ratios ± 95% C.I. (ppb)	4.0 ± 0.7	0.7 ± 0.2	0.2 ± 0.05	0.1 ± 0.03	0.1 ± 0.03	5.1
	Mixing ratios percentage (%)	15.3	2.7	0.9	0.6	0.4	20.0
	OFP ± 95% C.I. (ppb)	**34.5 ± 6.1**	**7.8 ± 1.8**	**2.3 ± 0.5**	**2.2 ± 0.5**	**1.7 ± 0.4**	**48.5**
	OFP percentage (%)	**45.5**	**10.2**	**3.0**	**3.0**	**2.2**	**63.9**
WQS (n = 74)	Mean mixing ratios ± 95% C.I. (ppb)	3.6 ± 0.3	0.6 ± 0.08	0.4 ± 0.03	0.2 ± 0.02	0.2 ± 0.02	5.0
	Mixing ratios percentage (%)	8.1	1.4	0.8	0.5	0.4	11.2
	OFP ± 95% C.I. (ppb)	**31.6 ± 2.9**	**7.0 ± 1.0**	**3.5 ± 0.3**	**3.3 ± 0.3**	**2.7 ± 0.2**	**48.1**
	OFP percentage (%)	**24.8**	**5.5**	**2.7**	**2.6**	**2.2**	**37.7**

[a] MIR values from Carter (2009).
[b] Rate constants with OH (K_{OH}) of VOCs from Atkinson et al. (1997) and Atkinson and Arey (2003).
[c] The alkenes lifetimes are based on OH rate constants from Atkinson and Arey (2003) and assume a 12-h daytime average OH concentration of 2×10^6 molecule cm^{-3} (Hofzumahaus et al., 2009).

upwind rural ZC (3.9 ± 0.7) or downwind rural WQS (3.6 ± 0.3 ppb), but had no significant difference when compared to those at suburban HEMC site (5.0 ± 0.8 ppb). Propylene ranked second among all alkenes. GEMC (1.5 ± 0.3 ppb) and HEMC (1.5 ± 0.4 ppb) sites all showed significantly higher levels of propylene ($p < 0.01$) than that at WQS (0.6 ± 0.1 ppb) or ZC (0.7 ± 0.2 ppb). Butenes (including 1-butene, trans-2-butene, and cis-2-butene) had much lower mixing ratios, less than 3% of the total NMHCs.

### 3.2. OH reactivity and ozone formation potentials (OFPs)

Hydroxyl radical (OH) is the dominant oxidant in the troposphere that controls the chemical lifetimes of many important trace gases (Levy, 1971; Ehhalt et al., 1998). Also OH is involved in the oxidation of VOCs that leads to the formation of tropospheric ozone and secondary organic aerosol (SOA) (Brasseur et al., 2003), and thus among numerous OH sinks VOCs are the most significant. OH reactivity, calculated as the product of the rate constant with OH and the mixing ratio, is widely

Fig. 2. Group compositions (mixing ratios) in percentages for NMHCs as well as their shares in OFPs and OH reactivity.

used as an estimate of the potential to consume OH for a single VOC (Kleinman et al., 2000, 2005; Lou et al., 2010):

$$VOC_R = \sum K_i [VOC]_i \qquad (1)$$

where k_i is the rate constant for reaction of OH with VOC_i. Reaction rate constants are from Atkinson et al. (1997) and Atkinson and Arey (2003). The anthropogenic VOCs observed in this study had total OH reactivity from 1.2 s^{-1} to 23.1 s^{-1}, with averages of 8.7 ± 0.8, 7.0 ± 1.1, 3.8 ± 0.6 and 7.0 ± 0.8 s^{-1} at GEMC, HEMC, ZC and WQS, respectively. Since reactive species like formaldehyde were not included in our calculation, these values were lower than those measured by laser flash photolysis and laser-induced fluorescence (LP-LIF) technique in the PRD region (10–120 s^{-1}; Lou et al., 2010) and Beijing (10–30 s^{-1}; Lu et al., 2013) in 2006, or that of 30 s^{-1} measured using a laser-induced pump and probe technique in urban Tokyo (Yoshino et al., 2012). The C_2–C_4 alkenes were found to be the VOC group that consume a larger portion of OH than the others (Fig. 2); they accounted for 38%, 48%, 50%, and 30% of the total OH reactivity by anthropogenic NMHCs at GEMC, HEMC, ZC and WQS, respectively. Only at WQS did aromatic hydrocarbons have higher OH reactivity (2.4 s^{-1}) than the C_2–C_4 alkenes (2.1 s^{-1}). Specifically, ethylene and propylene were the top two VOCs in OH reactivity at GEMC, HEMC and ZC; they altogether contributed over 25% of the OH reactivity by VOCs at the three sites. At WQS, however, OH reactivity of ethylene (0.8 ± 0.1 s^{-1}) ranked second to toluene (0.9 ± 0.1 s^{-1}), probably due to the heavy influence of solvents' emissions from upwind industrial areas and/or the faster decay of alkenes than aromatic hydrocarbons during their transport.

OFPs of C_2–C_4 alkenes and other NMHCs, calculated as the product of the average mixing ratios and the maximum incremental reactivity coefficient (MIR) of each compound (Carter, 2009), are also listed in Table 2. The total OFPs of NMHCs were 157 ± 20, 130 ± 20, 76 ± 12 and 127 ± 13 ppb at GEMC, HEMC, ZC and WQS, respectively. Ethylene ranked No. 1 by OFP and was shared 29.9%, 33.4%, 45.5% and 24.8% of total OFPs at GEMC, HEMC, ZC and WQS, respectively. Propylene ranked second at all sites except at WQS, where toluene had a larger portion (19.8%) than propylene (5.5%). As mentioned above, WQS is a site that might be influenced by the industrial emission of aromatic hydrocarbons in upwind Dongguan, an industrial city in the PRD region (Barletta et al., 2008; Chan et al., 2006; Y.L. Zhang et al., 2012).
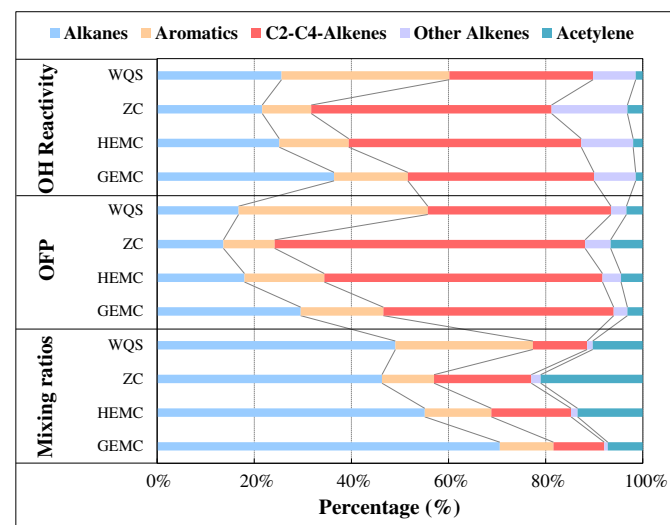
As showed in Fig. 2, C_2–C_4 alkenes shared only 11%–20% in mixing ratios of NMHCs, but accounted for 47.4%, 57.3% and 63.9% of OFPs at GEMC, HEMC and ZC, respectively; and only at WQS site did aromatic hydrocarbons (39.0%) have comparable contribution as C_2–C_4 alkenes (37.7%). It is worth noting that larger contribution of C_2–C_4 alkenes to ozone formation, particularly ethylene, has long been a problem in Asian cities (Barletta et al., 2002; So and Wang, 2004; Tang et al., 2007).

3.3. Source implication by the relationships with typical tracers

Table 3 lists the correlation coefficients of C_2–C_4 alkenes with typical tracers of various emission sources, including acetylene, propane, n-butane, i-pentane, benzene and toluene. Acetylene is a typical tracer of combustion sources (Barletta et al., 2005; Tang et al., 2009). Propane, n-butane, and i-butane are major components of LPG leakage or combustion (Blake and Rowland, 1995; Barletta et al., 2002). Gasoline evaporation would contribute substantially to ambient i-pentane (Zhang et al., 2013b). Benzene, as a carcinogenic compound forbidden to be used in industry, was mainly from automobile exhausts in urban area (Zhao et al., 2004; Barletta et al., 2008; Tang et al., 2008) and mainly from biomass burning in rural areas (Holzinger et al., 2001). Toluene was widely used as solvents in painting, coating, printing and cleaning processes in the highly industrialized PRD region (Chan et al., 2006; Y.L. Zhang et al., 2012) while vehicle exhaust is also an important source for toluene in urban areas (Barletta et al., 2008).

Both ethylene and propene showed significant correlations with acetylene at all four sites (Table 3), suggesting that they might have combustion-related sources. A weak correlation between ethylene and i-pentane even at the urban site GEMC (Table 3) indicates minor contribution of ethylene from gasoline evaporation. Significant correlations between ethylene and benzene at GEMC, HEMC and WQS ($r^2 = 0.25$–0.55, $p < 0.001$) suggest contribution of ethylene from vehicle exhausts, and similarly, correlations between ethylene and toluene at HEMC, ZC and WQS ($r^2 = 0.27$–0.61, $p < 0.001$) could be explained by emission of ethylene from industry activities. As HEMC lies about 10 km downwind the Guangzhou Petrochemical Co., which had an annual ethylene production of about 200,000 tons, ethylene at HEMC showed much better correlations with toluene largely due to input from petrochemical industry.

Propene showed better correlation with acetylene at GEMC and WQS than at HEMC and ZC (Table 3), indicating sources other than combustion at HEMC and ZC. Significant correlations between propene and propane at all sites, particularly at urban site GEMC, suggest contribution from LPG combustion or leakage. Propene is a widely used chemical feedstock to produce polypropylene plastics, and it also showed significant correlation with toluene at HEMC, ZC and WQS largely due to contribution from industry activities.

Butenes, including 1-butene, trans-2-butene and cis-2-butene, instead showed relatively weak correlations ($r^2 < 0.1$, $p > 0.05$) with acetylene particularly at ZC and WQS, indicating that butenes might have important sources other than combustion. However, both 1-butene and trans-2-butene had much better correlations with n-butane ($r^2 = 0.53$–0.98, $p < 0.001$) and i-butane ($r^2 = 0.40$–0.98, $p < 0.001$), which are mainly related to LPG leakage. Correlations of 1-butene, trans-2-butene and cis-2-butene with i-pentane ($r^2 = 0.56$–0.58, $p < 0.01$) at ZC site (Table 3) are indicative of input of gasoline evaporation, and only slight correlations of butenes with benzene ($r^2 = 0.26$, $p < 0.01$) were observed at ZC.

3.4. Source attribution by PMF

As alkenes are highly reactive when compared to AHs, source apportioning of alkenes based on their ambient levels from field campaigns is still a formidable task as compositions of alkenes may change drastically due to chemical aging during transport from emission sources to receptor sites. Although Shao et al. (2009) attempted to restore initial ratios to indicate sources of VOCs, there still existed large uncertainties since an individual VOC species in ambient air may vary greatly in where and when it was emitted to the atmosphere. Some paired VOCs, like trans-2-butene/cis-2-butene and m,p-xylenes/ethylbenzene, share common sources but have different atmospheric lifetimes, so their slopes are frequently used as indicators of chemical aging (Liu et al., 2009; Yuan et al., 2012; Y.J. Zhang et al., 2012). Moreover, the ratios of trans-2-butene to cis-2-butene from different emission sources are within a narrow range: they are 1.13–1.37 from gasoline evaporation (Zhang et al., 2013b), 1.2–1.45 from gasoline vehicle exhaust (Liu et al., 2008b; Guo et al., 2011), 1.46 from biofuel burning and 0.8 from agriculture residue burning (Andreae and Merlet, 2001), and 1.88 from pine combustion (Schauer et al., 2001). The scatter plots of trans-2-butene against cis-2-butene at the four sites (Fig. 3a) reveal quite similar slopes, which were 1.01, 1.16, 0.88 and 1.32, respectively, at GEMC, HEMC, WQS and ZC. It is worth noting that trans-2-butene

Table 3
Correlations between C_2–C_4 alkenes and typical tracers of emission sources.

| Sites	Species	Acetylene		Propane		n-Butane		i-Pentane		Benzene		Toluene	
		r^2	p	r^2	p	r^2	p	r^2	p	r^2	p	r^2	p
GEMC	Ethylene	0.62	<0.001	0.59	<0.001	0.38	<0.001	0.17	<0.01	0.25	<0.001	0.16	<0.05
	Propene	0.64	<0.001	0.64	<0.001	0.49	<0.001	0.23	<0.01	0.19	<0.01	0.21	<0.01
	1-Butene	0.17	<0.01	0.14	<0.01	0.41	<0.001	0.14	<0.05	n.a.	>0.05	0.12	<0.05
	Trans-2-butene	0.24	<0.001	0.12	<0.05	0.49	<0.001	0.14	<0.05	0.12	<0.05	0.19	<0.01
	Cis-2-butene	0.16	<0.01	0.10	<0.05	0.44	<0.001	0.10	<0.05	n.a.	>0.05	0.14	<0.05
HEMC	Ethylene	0.69	<0.001	0.58	<0.001	0.11	<0.05	0.14	<0.01	0.34	<0.001	0.61	<0.001
	Propene	0.36	<0.001	0.40	<0.001	0.10	<0.05	0.35	<0.01	0.25	<0.001	0.41	<0.001
	1-Butene	n.a.[a]	>0.05	0.18	<0.01	0.81	<0.001	0.17	<0.01	0.15	<0.01	n.a.	>0.05
	Trans-2-butene	0.10	<0.05	0.40	<0.001	0.76	<0.001	0.30	<0.001	0.28	<0.001	0.18	<0.05
	Cis-2-butene	0.06	>0.05	0.30	<0.001	0.90	<0.001	0.20	<0.001	0.26	<0.001	0.11	<0.05
ZC	Ethylene	0.74	<0.001	0.16	<0.05	n.a.	>0.05	n.a.	>0.05	0.05	>0.05	0.27	<0.001
	Propene	0.36	<0.001	0.35	<0.001	0.01	>0.05	0.10	<0.05	0.18	<0.01	0.66	<0.001
	1-Butene	n.a.	>0.05	0.34	<0.001	0.98	<0.001	0.58	<0.001	0.26	<0.001	0.10	>0.05
	Trans-2-butene	n.a.	>0.05	0.36	<0.001	0.98	<0.001	0.56	<0.001	0.26	<0.001	0.10	<0.05
	Cis-2-butene	n.a.	>0.05	0.36	<0.001	0.98	<0.001	0.56	<0.001	0.26	<0.001	0.10	>0.05
WQS	Ethylene	0.74	<0.001	0.35	<0.001	n.a.	>0.05	n.a.	<0.05	0.55	<0.001	0.31	<0.001
	Propene	0.59	<0.001	0.42	<0.001	n.a.	>0.05	0.25	<0.001	0.61	<0.001	0.26	<0.001
	1-Butene	n.a.	>0.05	n.a.	<0.05	0.53	<0.001	n.a.	>0.05	n.a.	>0.05	n.a.	>0.05
	Trans-2-butene	n.a.	>0.05	n.a.	>0.05	0.40	<0.001	n.a.	>0.05	n.a.	>0.05	n.a.	>0.05
	Cis-2-butene	n.a.	>0.05	n.a.	<0.05	0.79	<0.001	n.a.	>0.05	n.a.	>0.05	n.a.	>0.05

[a] n.a.: Correlation coefficients less than 0.1.
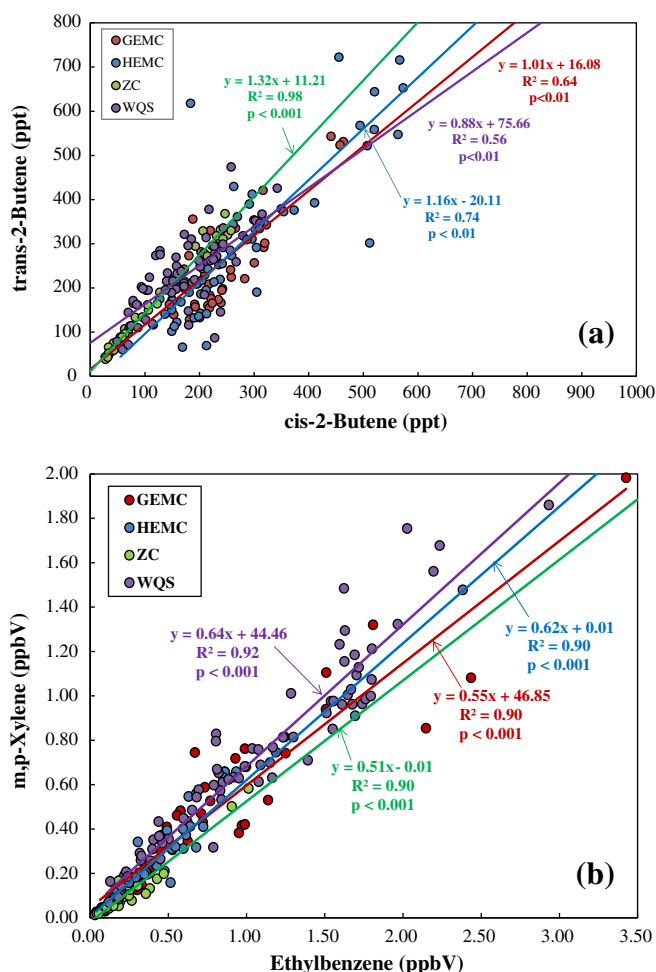
Fig. 3. Scatter plots of (a) trans-2-butene versus cis-2-butene; and (b) m,p-xylenes versus ethylbenzene at GEMC, HEMC, ZC and WQS.

to cis-2-butene at upwind ZC showed not only best correlation but also the highest slope (1.32) that fell right in the middle of vehicle exhausts (1.2–1.45; Liu et al., 2008b; Guo et al., 2011), suggesting relatively fresh input of vehicle exhausts. Also the slopes of m,p-xylenes against ethylbenzene (Fig. 3b) varied from 0.51 to 0.64. These similar slopes might reflect that there was not big difference in the degree of aging for the reactive VOCs among the four sites. The 26 most abundant NMHCs, including alkanes, alkenes, AHs, methyl tert-butyl ether (MTBE), trichloroethylene (TrCE), and tetrachloroethylene (TeCE) were selected for the PMF modeling. Five anthropogenic emission sources, namely vehicle exhausts, LPG, industrial processes losses, oil evaporation and biomass burning were resolved and typical factor profiles are shown in Fig. 4. The source of industrial process losses is characterized by a significant amount of AHs, n-hexane, TrCE and TeCE which are major components in various solvents commonly used in manufacturing industries, such as n-hexane in electronics industry particularly in the PRD region (Chan et al., 2006). LPG related emissions were identified by a dominance of propane, i-butane, n-butane and ethane, which are typical tracer of LPG-related emission (Barletta et al., 2008). Vehicle exhaust is identified by a significant presence of acetylene, C_4–C_6 alkanes and aromatics (Yuan et al., 2009). Furthermore, MTBE, a gasoline additive and unambiguous indicator for gasoline vehicle exhaust emissions (Chang et al., 2003), also contributed most in this factor. Biomass burning was also judged to be rich in acetylene, ethylene, and C_3–C_4 alkenes (Andreae and Merlet, 2001). Oil evaporation is characterized by the abundance of i-pentane and C_5–C_6 alkanes (Na et al., 2004; Zhang et al., 2013b).

Specific contributions of different sources to ethylene, propene, 1-butene, trans-2-butene, and cis-2-butene based on PMF at the four sites are presented in Fig. 5. Vehicle exhaust and LPG are two major sources and they altogether accounted for 52–62%, 58–77%, 73–83%, 68–79%, and 73–84% of ethylene, propene, 1-butene, trans-2-butene and cis-2-butene, respectively. On average vehicle exhausts alone contributed 39%, 32%, 49% and 41% for ethylene, and 41%, 36%, 35% and 35% for propene at GEMC, HEMC, ZC and WQS, respectively. LPG related sources ranked the second with a share of 21% to ethylene at GEMC; however, industry processes losses ranked the second with shares of 23% and 22% to ethylene respectively at HEMC and WQS, a little bit higher than shares of 21% and 20% by LPG. Meanwhile at the upwind rural site ZC, biomass burning contributes (21%) to ethylene and industry process losses made up of ethylene emissions (15%). Oil evaporation contributed (17%) to ethylene at GEMC, significantly more than at other sites (2%–9%).

For propene, LPG was an important contributor accounting for 36%, 26%, 23% and 31% at GEMC, HEMC, ZC and WQS, respectively. Biomass burning at HEMC (19%) and to industrial process losses at ZC (20%) at WQS (19%) impacted propylene. LPG contributed most to 1-butene at all sites ranging from 40–65%, followed by vehicle exhausts with shares of 33%, 19%, 19% and 35% at GEMC, HEMC, ZC and WQS, respectively. Industrial processes losses, biomass burning, and oil evaporation altogether accounted 27%, 17%, 21% and 24% of 1-butene at GEMC, HEMC, ZC and WQS, respectively. Trans-2-butene and cis-2-butene showed very similar patterns in their sources (Fig. 5). The same as 1-butene, LPG related sources were the No. 1 contributor to trans-2-butene and cis-2-butene; it contributed 55%, 60%, 38% and 45% of trans-2-butene, and 56%, 62%, 40% and 49% of cis-2-butene, respectively, at GEMC, HEMC, ZC and WQS. Vehicle exhaust accounted for 19–33% of trans-2-butene and 20–36% of cis-2-butene. Contributions from industrial process losses were the least with percentages of 0.3–6% and 2–4% for trans-2-butene and cis-2-butene, respectively. Biomass burning and oil evaporation together accounted for 16–29% and 12–24% of trans-2-butene and cis-2-butene, respectively.

It is worth noting that LPG contributed substantially to the major alkenes, particularly propene and butenes. A main reason is that unlike LPG that has propane and butanes as dominant components (Blake and Rowland, 1995), LPG used in the PRD in 2009 was quite rich in light alkenes. Fig. 6 is a typical chromatography of the C_3–C_4 hydrocarbons of pipelined gas and its combustion products from a cooking stove. The high percentages of propenes and butenes in the LPG are great concern for their contribution to ozone formation if leaked, or emitted from incomplete combustion. Using this kind of alkene-rich LPG, probably oil cracking gas without further refining, would not influence its heating calorific value but is apparently not environmentally friendly for the ozone formation potentials. Therefore, LPG should be further refined to reduce its contents of alkenes before used as pipeline gas or it should be replaced by cleaner LNG, such as what is happening in Guangzhou. In fact, Guangdong province, of which Guangzhou is the capital city, accounted for more than 40% LPG consumption of the whole country in 2011. LPG used in Guangzhou for household pipelined gas was completely replaced by LNG before the 2010 Asian Games (Guangzhou; November 12–27, 2010). Furthermore, as announced by the Guangzhou government in 2012, the ~9000 buses and ~16,000 taxi powered by LPG in the public transport sector were planned to be gradually replaced by LNG-powered ones in the coming decade.

4. Conclusions

Monitoring of ambient VOCs at representative urban, suburban and rural sites during November–December 2009 in the PRD region revealed that C_2–C_4 light alkenes were predominant ozone formation precursors. C_2–C_4 alkenes were 10–20% in total mixing ratios of NMHCs but accounted for 46%, 58% and 65% of OFPs by NMHCs at GEMC, HEMC and ZC, respectively. At the WQS site, AHs contributed a slightly larger
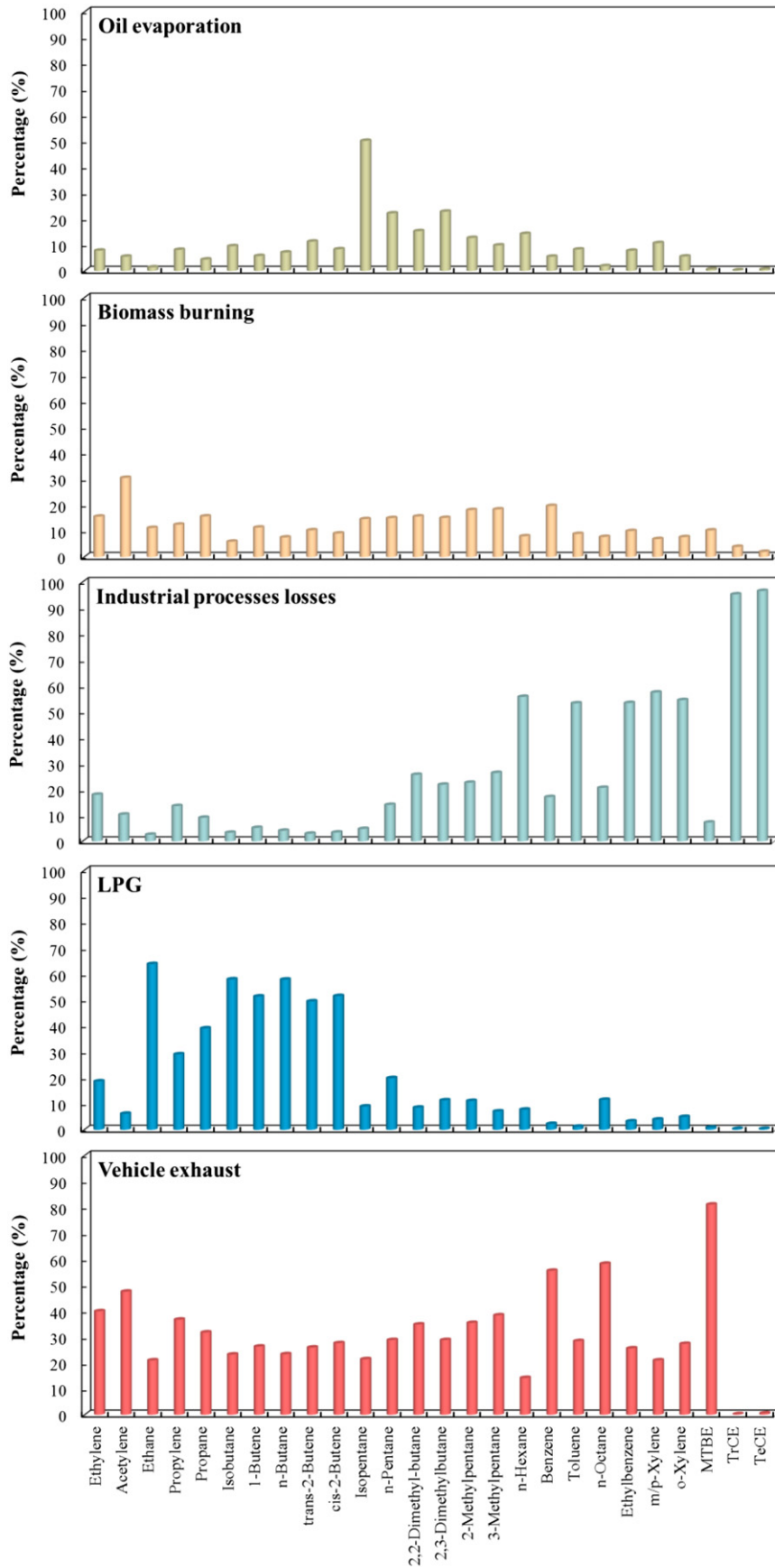
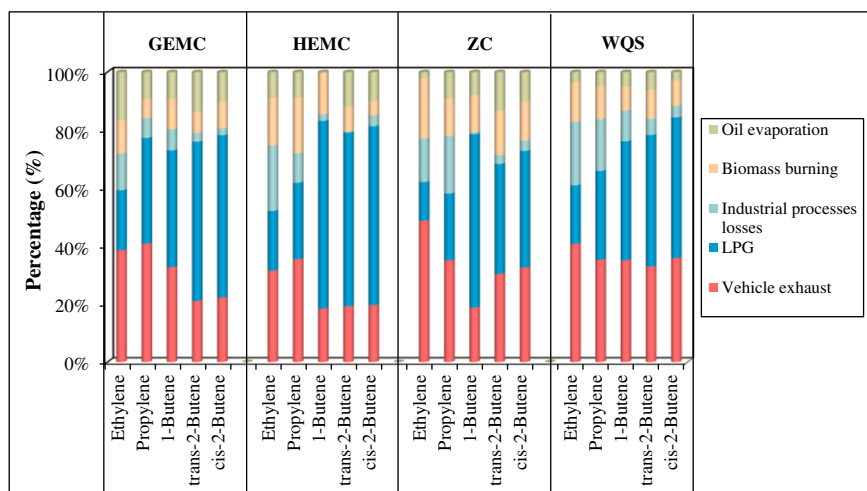**Fig. 4.** Factor profiles resolved by PMF.

Fig. 5. Source contributions for C_2–C_4 alkenes.

percentage (39%) in OFPs than C_2–C_4 alkenes (38%). Similarly, 38%, 48%, 50%, and 30% of the total OH reactivity by NMHCs were attributed to C_2–C_4 alkenes. Ethylene, as the most abundant alkene, made up 7–15% in

total mixing ratios of NMHCs and contributed 30%, 33%, 46% and 25% of OFPs at GEMC, HEMC, ZC and WQS, respectively. As surface ozone pollution is an increasing concern in the PRD region and ozone
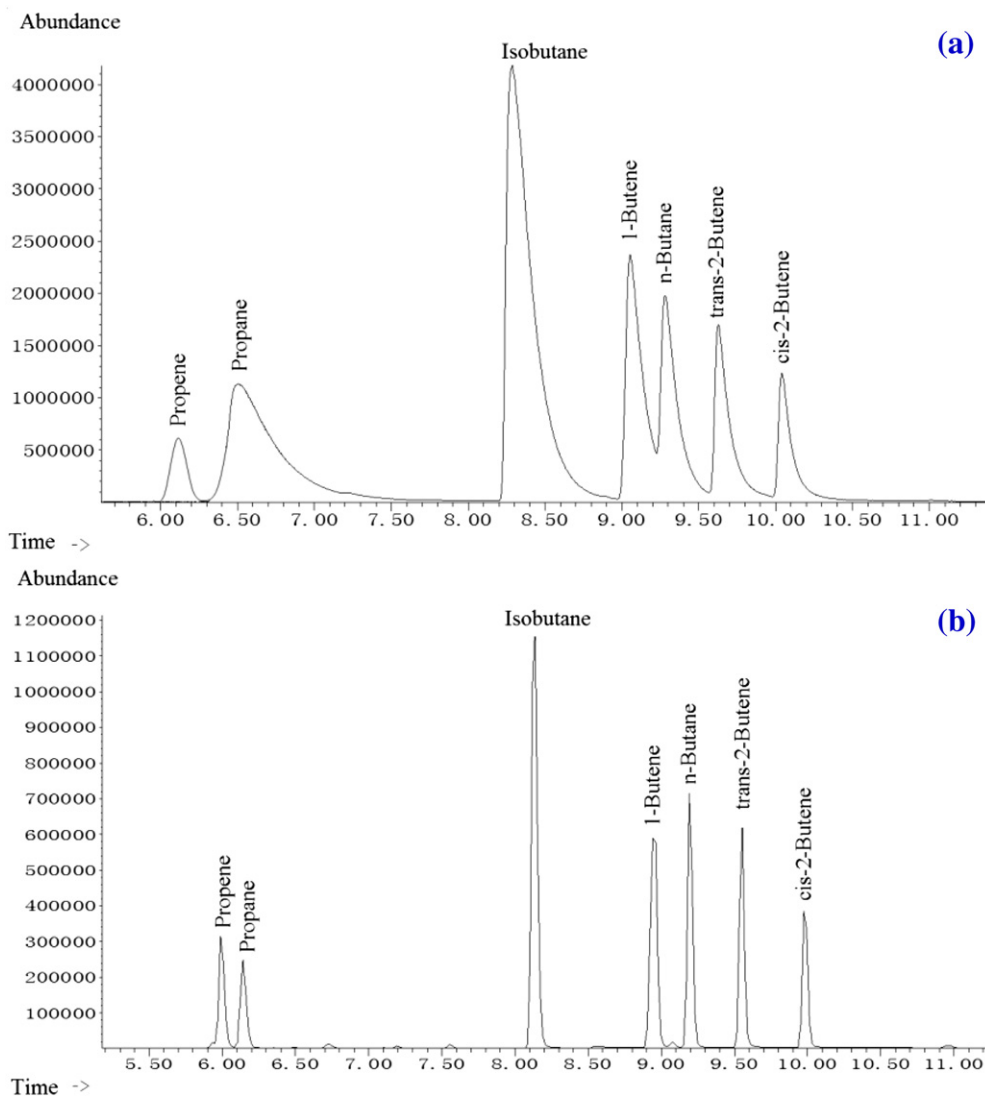

Fig. 6. C_3–C_4 hydrocarbons in (a) LPG then as pipeline gas and (b) plumes above domestic cooking stoves using LPG. Chromatogram (a) had poor peak separation due to heavy loads into the GC column after injecting samples without dilution.

production in the region was previously found sensitive to VOC emissions, our study suggests that reactive C_2–C_4 alkenes are significant ozone precursors that need to be reduced in this region.

Correlations between C_2–C_4 alkenes and typical tracers of emission sources suggested that ethylene might be largely related to vehicle exhausts and industry activities, while propene and butenes were much more impacted by LPG leakage or combustion. Further source apportioning with the PMF confirmed that vehicle exhausts and LPG were two major sources that altogether accounted for 52–62%, 58–77%, 73–83%, 68–79% and 73–84% for ethylene, propene, 1-butene, trans-2-butene, and cis-2-butene, respectively. Vehicle exhaust as the No. 1 contributor to ethylene and propene contributed 39%, 32%, 49% and 41% of ethylene, and 41%, 36% 35% and 35% of propene, respectively at GEMC, HEMC, ZC and WQS. LPG was the No. 1 contributor to butenes and also contributed substantially (23–36%) to propene. We conducted extensive analysis of VOCs in LPG used in 2009 as pipeline gas in Guangzhou, as well as VOCs from domestic cooking stoves using LPG. The results confirmed that fractions of propene and butenes are present at high concentrations in the pipeline gas so that its leakage or incomplete combustion would contribute to ambient alkenes as ozone precursors. Thus, limiting the content of alkenes in LPG would benefit the control of ozone pollution in the region.

Acknowledgments

References

Anderson MJ, Miller SL, Milford JB. Source apportionment of exposure to toxic volatile organic compounds using positive matrix factorization. J Expo Anal Environ Epidemiol 2001;11:295–307.

Andreae MO, Merlet P. Emission of trace gases and aerosols from biomass burning. Global Biogeochem Cycles 2001;15:955–66.

Atkinson R, Arey J. Atmospheric degradation of volatile organic compounds. Chem Rev 2003;103:4605–38.

Atkinson R, Baulch DL, Cox RA, Hampson Jr RF, Kerr JA, Rossi MJ, et al. Evaluated kinetic and photochemical data for atmospheric chemistry: supplement VI. J Phys Chem Ref Data 1997;26:1329–499.

Barletta B, Meinardi S, Simpson IJ, Khwaja HA, Blake DR, Rowland FS. Mixing ratios of volatile organic compounds (VOCs) in the atmosphere of Karachi, Pakistan. Atmos Environ 2002;36:3429–43.

Barletta B, Meinardi S, Rowland FS, Chan CY, Wang XM, Zou SC, et al. Volatile organic compounds in 43 Chinese cities. Atmos Environ 2005;39:5979–90.

Barletta B, Meinardi S, Simpson IJ, Zou S, Rowland FS, Blake DR. Ambient mixing ratios of nonmethane hydrocarbons (NMHCs) in two major urban centers of the Pearl River Delta (PRD) region: Guangzhou and Dongguan. Atmos Environ 2008;42:4393–408.

Beckett WS. Ozone, air-pollution, and respiratory health. Yale J Biol Med 1991;64:167–75.

Beig G, Singh V. Trends in tropical tropospheric column ozone from satellite data and MOZART model. Geophys Res Lett 2007;34.

Blake DR, Rowland FS. Urban leakage of liquefied petroleum gas and its impact on Mexico City air-quality. Science 1995;269:953–6.

Brasseur GP, Prinn RG, Pszenny AP, editors. Atmospheric chemistry in a changing world. The IGBP seriesBerlin, Germany: Springer; 2003.

Brown SG, Frankel A, Hafner HR. Source apportionment of VOCs in the Los Angeles area using positive matrix factorization. Atmos Environ 2007;41:227–37.

Carter WPL. Update maximum incremental reactivity scale and hydrocarbon bin reactivities for regulatory application. California Air Resources Board, Contract 07-339; 2009.

Chameides WL, Kasibhatla PS, Yienger J, Levy H. Growth of continental-scale metro-agroplexes, regional ozone pollution, and world food-production. Science 1994;264:74–7.

Chan CY, Chan LY, Harris JM. Urban and background ozone trend in 1984–1999 at subtropical Hong Kong, South China. Ozone Sci Eng 2003;25:513–22.

Chan LY, Chu KW, Zou SC, Chan CY, Wang XM, Barletta B, et al. Characteristics of nonmethane hydrocarbons (NMHCs) in industrial, industrial-urban, and industrial-suburban atmospheres of the Pearl River Delta (PRD) region of south China. J Geophys Res 2006;111.

Chang CC, Lo SJ, Lo JG, Wang JL. Analysis of methyl tert-butyl ether in the atmosphere and implications as an exclusive indicator of automobile exhaust. Atmos Environ 2003; 37:4747–55.

Cheng H, Guo H, Wang X, Saunders S, Lam SHM, Jiang F, et al. On the relationship between ozone and its precursors in the Pearl River Delta: application of an observation-based model (OBM). Environ Sci Pollut Res 2010;17:547–60.

Dodge MC. Combined use of modeling techniques and smog chamber data to derive ozone-precursor relationships. In: Dimitriades B, editor. Proceedings of the international conference on photochemical oxidant pollution and its control, vol. II. EPA-600/3-77-001b; 1977.

Ehhalt DH, Rohrer F, Wahner A, Prather MJ, Blake DR. On the use of hydrocarbons for the determination of tropospheric OH concentrations. J Geophys Res 1998;103.

Finlayson-Pitts BJ. Atmospheric chemistry. Proc Natl Acad Sci 2010;107.

Finlayson-Pitts BJ, Pitts Jr JN. Volatile organic compounds: ozone formation, alternative fuels, and toxics. Chem Ind 1993;18.

Finlayson-Pitts BJ, Pitts Jr JN. Chemistry of the upper and lower atmosphere. Academic Press; 1999 [Chapter 16].

Guo H, Wang T, Blake DR, Simpson IJ, Kwok YH, Li YS. Regional and local contributions to ambient non-methane volatile organic compounds at a polluted rural/coastal site in Pearl River Delta, China. Atmos Environ 2006;40:2345–59.

Guo H, Zou SC, Tsai WY, Chan LY, Blake DR. Emission characteristics of nonmethane hydrocarbons from private cars and taxis at different driving speeds in Hong Kong. Atmos Environ 2011;45:2711–21.

Haagen-smit AJ, Fox MM. Ozone formation in photochemical oxidation of organic substances. Ind Eng Chem 1956;48:1484–7.

Hakami A, Seinfeld JH, Chai TF, Tang YH, Carmichael GR, Sandu A. Adjoint sensitivity analysis of ozone nonattainment over the continental United States. Environ Sci Technol 2006;40:3855–64.

Hofzumahaus A, Rohrer F, Lu K, Bohn B, Brauers T, Chang CC, et al. Amplified trace gas removal in the troposphere. Science 2009;324:1702–4.

Holzinger R, Kleiss B, Donoso L, Sanhueza E. Aromatic hydrocarbons at urban, sub-urban, rural (8°52′N; 67°19′W) and remote sites in Venezuela. Atmos Environ 2001;35: 4917–27.

Hopke PK, Ramadan Z, Paatero P, Norris GA, Landis MS, Williams RW, et al. Receptor modeling of ambient and personal exposure samples: 1998 Baltimore particulate matter epidemiology-exposure study. Atmos Environ 2003;37:3289–302.

Intergovernmental Panel on Climate Change (IPCC). Contribution of Working Group I to the Fourth Assessment Report of the Intergovernmental Panel on Climate Change. In: Solomon S, Qin D, Manning M, Chen Z, Marquis M, Averyt KB, Tignor M, Miller HL, editors. Cambridge, United Kingdom and New York, NY, USA: Cambridge University Press; 2007.

Kleinman LI, Daum PH, Imre D, Lee JH, Lee YN, Nunnemacker LJ, et al. Ozone production in the New York City urban plume. J Geophys Res 2000;105:14,495–511.

Kleinman LI, Daum PH, Lee YN, Nunnermacker LJ, Springston SR, Weinstein-Lloyd J, et al. A comparative study of ozone production in five U.S. metropolitan areas. J Geophys Res 2005;110.

Kulkarni PS, Ghude SD, Bortoli D. Tropospheric ozone (TOR) trend over three major inland Indian cities: Delhi, Hyderabad and Bangalore. Ann Geophys 2010;28:1879–85.

Lal DM, Ghude SD, Patil SD, Kulkarni SH, Jena C, Tiwari S, et al. Tropospheric ozone and aerosol long-term trends over the Indo-Gangetic Plain (IGP), India. Atmos Res 2012;116:82–92.

Lam KS, Wang TJ, Wu CL, Li YS. Study on an ozone episode in hot season in Hong Kong and transboundary air pollution over Pearl River Delta region of China. Atmos Environ 2005;39:1967–77.

Levy H. Normal atmosphere: large radical and formaldehyde concentrations predicted. Science 1971;173:141–3.

Lippmann M. Health-effects of ozone — a critical-review. J Air Waste Manage Assoc 1989; 39:672–95.

Liu Y, Shao M, Lu S, Chang CC, Wang JL, Fu L. Source apportionment of ambient volatile organic compounds in the Pearl River Delta, China: part II. Atmos Environ 2008a; 42:6261–74.

Liu Y, Shao M, Fu L, Lu S, Zeng L, Tang D. Source profiles of volatile organic compounds (VOCs) measured in China: part I. Atmos Environ 2008b;42:6247–60.

Liu J, Mu Y, Zhang Y, Zhang Z, Wang X, Liu Y, et al. Atmospheric levels of BTEX compounds during the 2008 Olympic Games in the urban area of Beijing. Sci Total Environ 2009; 408:109–16.

Liu Z, Wang Y, Gu D, Zhao C, Huey LG, Stickel R, et al. Summertime photochemistry during CAREBeijing-2007: RO$_x$ budgets and O$_3$ formation. Atmos Chem Phys 2012;12: 7737–52.

Logan JA. Tropospheric ozone — seasonal behavior, trends, and anthropogenic influence. J Geophys Res 1985;90:10463–82.

Lou S, Holland F, Rohrer F, Lu K, Bohn B, Brauers T, et al. Atmospheric OH reactivities in the Pearl River Delta — China in summer 2006: measurement and model results. Atmos Chem Phys 2010;10:11243–60.

Lu KD, Hofzumahaus A, Holland F, Bohn B, Brauers T, Fuchs H, et al. Missing OH source in a suburban environment near Beijing: observed and modelled OH and HO$_2$ concentrations in summer 2006. Atmos Chem Phys 2013;13:1057–80.

Martinez JR, Maxwell C, Javitz HS, Bawol R. Performance evaluation of the Empirical Kinetic Modeling Approach (EKMA). Air pollution modeling and its application II NATO • challenges of modern society, volume 3; 1983. p. 199–211.

Na K, Kim YP, Moon I, Moon KC. Chemical composition of major VOC emission sources in the Seoul atmosphere. Chemosphere 2004;55:585–94.

Paatero P. Least squares formulation of robust non-negative factor analysis. Chemometr Intell Lab 1997;37:23–35.

Paatero P, Tapper U. Positive matrix factorization — a nonnegative factor model with optimal utilization of error-estimates of data values. Environmetrics 1994;5: 111–26.

Poirot RL, Wishinski PR, Hopke PK, Polissar AV. Comparative application of multiple receptor methods to identify aerosol sources in northern Vermont. Environ Sci Technol 2001;35:4622–36.

Polissar AV, Hopke PK, Paatero P. Atmospheric aerosol over Alaska — 2. Elemental composition and sources. J Geophys Res 1998;103:19045–57.

Reff A, Eberly SI, Bhave PV. Receptor modeling of ambient particulate matter data using positive matrix factorization: review of existing methods. J Air Waste Manage Assoc 2007;57:146–54.

Schauer JJ, Kleeman MJ, Cass GR, Simoneit BRT. Measurement of emissions from air pollution sources. 3. C1–C29 organic compounds from fireplace combustion of wood. Environ Sci Technol 2001;35:1716–28.

Shao M, Lu S, Liu Y, Xie X, Chang C, Huang S, et al. Volatile organic compounds measured in summer in Beijing and their role in ground-level ozone formation. J Geophys Res 2009;114.

So KL, Wang T. C3–C12 non-methane hydrocarbons in subtropical Hong Kong: spatial–temporal variations, source–receptor relationships and photochemical reactivity. Sci Total Environ 2004;328:161–74.

Tang JH, Chan LY, Chan CY, Li YS, Chang CC, Liu SC, et al. Characteristics and diurnal variations of NMHCs at urban, suburban, and rural sites in the Pearl River Delta and a remote site in South China. Atmos Environ 2007;41:8620–32.

Tang JH, Chan LY, Chan CY, Li YS, Chang CC, Wang XM, et al. Implications of changing urban and rural emissions on non-methane hydrocarbons in the Pearl River Delta region of China. Atmos Environ 2008;42:3780–94.

Tang JH, Chan LY, Chan CY, Liu SC, Li YS. Characteristics and sources of non-methane hydrocarbons in background atmospheres of eastern, southwestern, and southern China. J Geophys Res 2009;114.

Wang X, Lu W, Wang W, Leung AYT. A study of ozone variation trend within area of affecting human health in Hong Kong. Chemosphere 2003;52:1405–10.

Wang X, Manning W, Feng Z, Zhu Y. Ground-level ozone in China: distribution and effects on crop yields. Environ Pollut 2007a;147:394–400.

Wang X, Zheng Q, Yao F, Chen Z, Feng Z, Manning WJ. Assessing the impact of ambient ozone on growth and yield of a rice (*Oryza sativa* L.) and a wheat (*Triticum aestivum* L.) cultivar grown in the Yangtze Delta, China, using three rates of application of ethylenediurea (EDU). Environ Pollut 2007b;148:390–5.

Wang T, Wei XL, Ding AJ, Poon CN, Lam KS, Li YS, et al. Increasing surface ozone concentrations in the background atmosphere of Southern China, 1994–2007. Atmos Chem Phys 2009;9:6217–27.

Yoshino A, Nakashima Y, Miyazaki K, Kato S, Suthawaree J, Shimo N, et al. Air quality diagnosis from comprehensive observations of total OH reactivity and reactive trace species in urban central Tokyo. Atmos Environ 2012;49:51–9.

Yuan Z, Lau AKH, Shao M, Louie PKK, Liu SC, Zhu T. Source analysis of volatile organic compounds by positive matrix factorization in urban and rural environments in Beijing. J Geophys Res 2009;114.

Yuan B, Chen W, Shao M, Wang M, Lu S, Wang B, et al. Measurements of ambient hydrocarbons and carbonyls in the Pearl River Delta (PRD), China. Atmos Res 2012;116: 93–104.

Zhang J, Wang T, Chameides WL, Cardelino C, Kwok J, Blake DR, et al. Ozone production and hydrocarbon reactivity in Hong Kong, Southern China. Atmos Chem Phys 2007; 7:557–73.

Zhang YJ, Mu Y, Liang P, Xu Z, Liu J, Zhang H, et al. Atmospheric BTEX and carbonyls during summer seasons of 2008–2010 in Beijing. Atmos Environ 2012a;59:186–91.

Zhang YL, Wang XM, Blake DR, Li L, Zhang Z, Wang S, et al. Aromatic hydrocarbons as ozone precursors before and after outbreak of the 2008 financial crisis in the Pearl River Delta region, south China. J Geophys Res 2012b;117.

Zhang YL, Wang XM, Barletta B, Simpson IJ, Blake DR, Fu X, et al. Source attributions of hazardous aromatic hydrocarbons in urban, suburban and rural areas in the Pearl River Delta (PRD) region. J Hazard Mater 2013a;250:403–11.

Zhang YL, Wang XM, Zhang Z, Lu S, Shao M, Lee FSC, et al. Species profiles and normalized reactivity of volatile organic compounds from gasoline evaporation in China. Atmos Environ 2013b;79:110–8.

Zhao LR, Wang XM, He QS, Wang H, Sheng GY, Chan LY, et al. Exposure to hazardous volatile organic compounds, PM_{10} and CO while walking along streets in urban Guangzhou, China. Atmos Environ 2004;38:6177–84.

Zheng J, Zhong L, Wang T, Louie PKK, Li Z. Ground-level ozone in the Pearl River Delta region: analysis of data from a recently established regional air quality monitoring network. Atmos Environ 2010;44:814–23.